Operational Envelope of a 150 kW Huels Type Arc-jet

Jae-Jeong Na*† · Kwan-Ho Moon* · Yun-Ky Hong* · Seung-Wook Baek** · Chul Park**

ABSTRACT

In this work, we introduce a newly constructed arc-jet device of 150 kW input power. The design of this device is a Huels type with a narrow downstream electrode. General features of this device are first described. From the measured values of electrical power input, heat discharged into cooling water, gas flow rate, and settling chamber pressure, average enthalpy was determined using the heat balance and sonic throat methods. Using the settling chamber pressure and average enthalpy values, the flow properties in the nozzle and the heat transfer rate to the stagnation point of a blunt body are calculated accounting for thermochemical nonequilibrium. The envelope of enthalpy, pressure, degree of dissociation, and heat transfer rate are presented. Stagnation temperature is predicted to be between 4630 to 6050 °K, and the stagnation point heat transfer rate is predicted to be between 175 and 318 W/cm^2 for a blunt body of 3 mm nose radius. Degree of dissociation in the stagnation region of the blunt body exceeds 30%.

Key Words : Hypersonic flow, Chemically reacting flow, Heat transfer, Plasma-jet.

기 호 설 명

h Enthalpy, J/kg	$\dot{\omega}_i$ Chemical source term of species i, kg/(m^3-sec)
$\dot{m}$ Mass flow rate, kg/sec	x Axial distance of nozzle, m
p Pressure. pascal	γ_i Mass fraction of species i
u Flow velocity, m/sec	ρ Flow density, kg/m^3
T_v Vibrational temperature, K	

1. Introduction

In the testing of the heat-resistant materials for satellite launch systems, high temperature synthesis of materials, waste treatment, and plasma processing, arc-jet, sometimes called plasma-jet, devices occupy an important position. In their use, the flow enthalpy and pressure become the two most important parameters. For instance, for synthesis of diamond, the flow enthalpy must be sufficiently high to produce 4500 K needed for vaporization of carbon in the settling chamber. A launch vehicle encounters an environment containing atomic oxygen which chemically interacts with the surface materials. To test such a surface, the device must produce dissociation of oxygen.

There are many different designs for an arc-jet. However, most such designs are for relatively small devices. For a large device, there are mainly two known types: Huels type and segmented constrictor type[1].

The Huels type arc-heater was developed in

* Graduate student, Department of aerospace engineering, Korea Advanced Institute of Science and Technology
** Professor, Department of aerospace engineering, Korea Advanced Institute of Science and Technology
† Jae-Jeong Na, njj7284@kaist.ac.kr

Germany by Chemische Huels in the late 1930's. The original design was further improved by Linde Corporation and McDonnell Douglas Research Laboratory in the United States. In the original design, two electrodes have the same relatively large diameter. A maximum enthalpy of about 5 MJ/kg was achieved. This relatively low enthalpy of this type device is a result of the relatively large inner diameter of the two electrodes. In subsequent improvements, the inner diameter of the downstream electrodes was made smaller, which led to higher ethalpies[2, 3]: the small downstream electrode reduces the mass flow rate and thereby raises flow enthalpy.

Segmented constrictor type arc-jet devices were developed through the effort of NASA to raise enthalpy. Enthalpies exceeding 20 MJ/kg have been achieved at settling chamber pressures of about 5 atm[1]. Such high enthalpies are produced by this device because of the relatively small flow passage between the electrodes. The main drawback of this type is its complexity and high cost of fabrication and maintenance.

In recent months, an effort was made by Korea Advanced Institute of Science and Technology (KAIST) to construct an arc-jet device of the improved Huels type. In this report, we describe the general features of this device. The experimental data taken to date and the performance values derived from these data are described. Theoretical calculation is performed for the flow through the nozzle and the flow in the stagnation region of a blunt body placed at the exit of this device. The operating envelope of this device derived through the experiment and theoretical calculation is then presented. It will be shown that this device produces an enthalpy sufficiently high for many applications, e.g., production of diamond.

2. Description of the 150 kW arc-jet

2.1 General features

Figure 1 shows the 150 kW arc-jet device constructed in this work. The primary purpose of this device is to test the performance of the heat-resistant materials used for space launch vehicles developed in Korea. Secondarily, materials processing, such as diamond synthesis, is planned. The inset shows the jet flow produced by the device in the atmosphere.

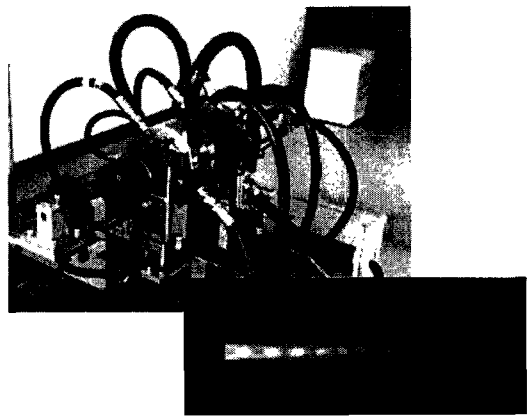

Fig. 1 150 kW arc-jet and nozzle exit flow.

Figure 2 shows the schematic of the device. As shown, two tandem cylindrical electrodes are separated by a central swirl air injection chamber and insulated electrically from each other. The 140 mm long upstream (rear) electrode has an inside diameter of 30 mm. A constrictor, which has an internal diameter of 15 mm and length of 50 mm is placed at the inlet of the 160 mm-long downstream electrode. A diverging nozzle is attached to the downstream end of the arc-jet to expand the flow to a supersonic velocity. For material synthesis, raw material will be injected in the settling chamber region which is the region immediately upstream of the nozzle throat.

The nozzle has a conical configuration, a throat diameter of 6 mm, exit diameter of 9 mm, cross-sectional throat area A_* of 28.3 mm^2, and an exit-to-throat area ratio of 2.27. The divergence angle is 12 degrees. The area ratio is chosen so that the flow emerging from the nozzle exit will have static pressure higher than the atmospheric pressure. This constraint exists at this time because there is no vacuum pumping system. (After the planned vacuum system is installed, a nozzle of a larger area ratio will be installed.) The settling chamber pressure p_{ch} is measured at the upstream end

wall (rear electrode). Because the diameter of the electrode (15 mm) is much larger than the throat diameter (6 mm), pressure is believed to be the same up the settling chamber region immediate upstream of the nozzle.

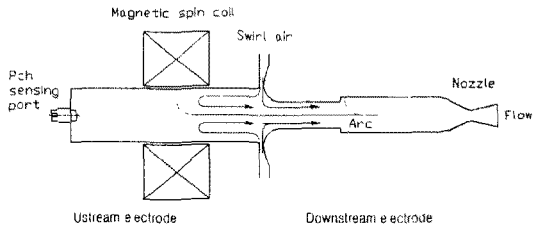

Fig. 2 Schematic of the KAIST 150 kW arc-jet

As shown in Fig. 2,. compressed air is injected tangentially from the gap between the two electrodes in a counter-clockwise direction looking downstream. The resultant radial pressure gradient is believed to stabilize the arc discharge. A magnetic spin coil is positioned over the rear electrode to rotate the arc termination. This is believed to prevent arc transfer to the rear plug. The constrictor on the downstream electrode reduces the flow rate and increases the enthalpy as in a segmented-constrictor type device. The constrictor is also believed to reduce the axial arc fluctuation caused by the aerodynamic effect occurring at the arc attachment point.

Figure 3 shows the schematic of the electrical circuit. As shown, the DC current passes through an induction coil of 200 kHz. The induction coil initiates ionization. The DC power supply is a three-phase rectifier system, and has a nominal power rating of 360 kW. A silicon-rectifier control (thyrister) system maintains the electrical current at a desired value regardless of the voltage between the electrodes. The arc current I, arc voltage E, and the settling chamber pressure p_{ch}, and mass flow rate through the device $\dot{m}$ are measured routinely. The electrodes, nozzle, and the magnetic spin coil are individually water-cooled and instrumented to determine the heat removed in these components. A cooling system supplies water of 10 kg/s flow rate at 20 atms. The power consumed by the cooling water system is 30 kW.

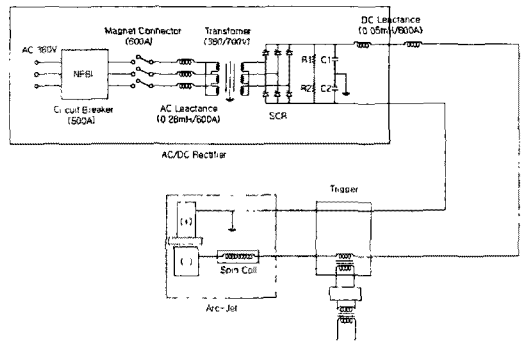

Fig. 3 Schematic of the electrical circuit

2.2 Pressure and average enthalpy

The average enthalpy of the flow produced by the device h_{av} is given by the relation

$$\dot{m} \times h_{av} = E \times I - \textit{Power removed in cooling water} \quad (1)$$

The procedure of determining h_{av} in this way is known as heat-balance method. The ratio

$$\eta = \dot{m} \times h_{av} / EI \quad (2)$$

is termed heater efficiency, and is an important parameter in an arc-jet device because the cost of synthesizing a material in the device is inversely proportional to this parameter. In a segmented constrictor type facility, this quantity is typically about 0.4. In the present work, h_{av} and associated η value are routinely measured.

Another well-known method of determining enthalpy is a method known as sonic-throat method. This method is based on the fact that, assuming that the flow through the nozzle is purely one-dimensional and that there is no boundary layer, the flow rate through the nozzle throat is proportional to the density and to the sonic speed of the flow in the settling chamber. Because the density and sonic speed are functions of settling chamber pressure and enthalpy, one can write a relationship among chamber pressure, enthalpy, and mass flow rate. For a perfect gas, this relationship is simple and involves a

square-root of enthalpy. For a real gas involving internal excitation, dissociation, and ionization, a thermochemical equilibrium relationship needs to be invoked. For air at high temperature, a semi-empirical relationship has been derived as[4]

$$\frac{\dot{m}}{A_* p_{ch}} = \frac{1.23 \cdot 10^{-3}}{h_{st}^{0.397}} \qquad (3)$$

Here, h_{st} signifies enthalpy by sonic-throat method. The power 0.397, in place of 0.5 for a perfect gas, results from the high temperature real-gas effect.

In principle, heat balance method is more straightforward than the sonic-throat method. However, measurement error is larger with the heat balance method because it involves many measured quantities. In the present device, h_{av} and h_{st} are found to be different by less than 8 %. Therefore, the following calculations have been carried out using the sonic-throat enthalpy h_{st}.

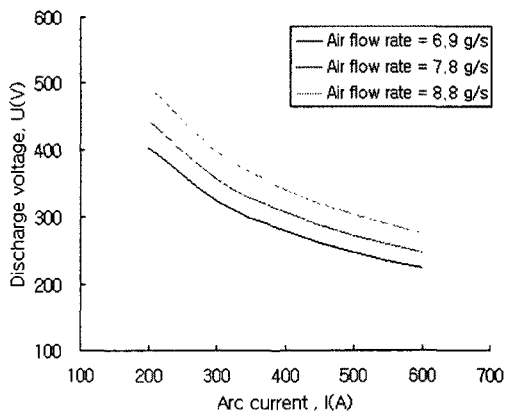

Fig. 4 Current-voltage relationship with the mass flow rate

Figure 4 shows the electrical current-voltage relationship with the mass flow rate ṁ as the parameter. One striking feature of this plot is the negative slop in the E-I curves. That is, the ohms law of fixed resistivity does not apply, and the device is ohmically negative. This ohmic negativity leads to an instability in electric discharge and also to a difficulty in control of current. This problem is overcome in the present facility by the use of the thyrister control system described above.

In Fig. 5(a), the operating envelope of the present device is shown in terms of chamber pressure p_{ch} and sonic-throat enthalpy h_{st}, As shown, the pressure ranges from 4 to 10 atm, and enthalpy ranges from 6 to 9 MJ/kg.

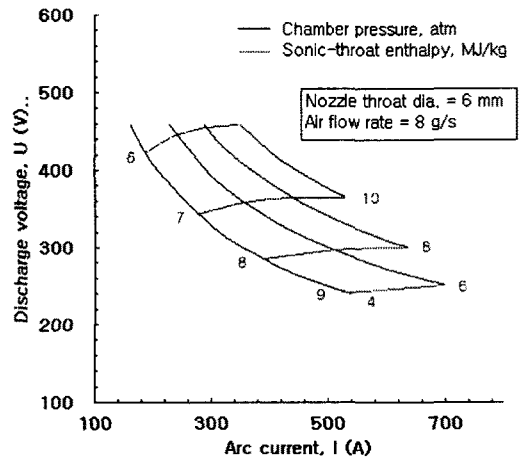

Fig. 5(a) Operating envelope in terms of chamber pressure p_{ch} and sonic-throat enthalpy h_{st}

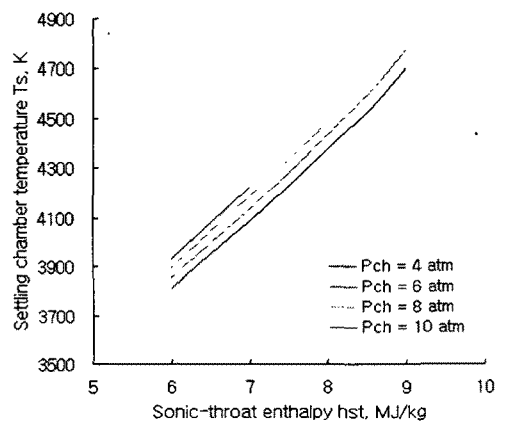

Fig. 5(b) Settling chamber temperature T_s corresponding to h_{st}

In Fig. 5(b), a similar plot is shown for the settling chamber temperature T_s corresponding to h_{st}. As seen, T_s exceeds 4500 °K needed for production of diamond. In Fig. 5(c), efficiency of the device is shown. The efficiency values

are higher than the typical segmented constrictor types. In Fig. 5(d), the operating envelope of the present device is compared with those of the Huels type devices and segmented constrictor type devices existing throughout the world[1]. As seen, the present operating range falls well within the range of existing facilities.

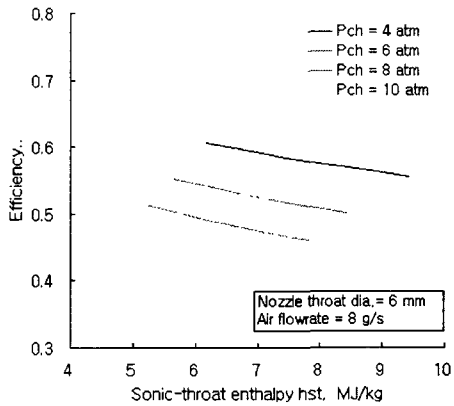

Fig. 5(c) Efficiency of 150 kW arc-jet

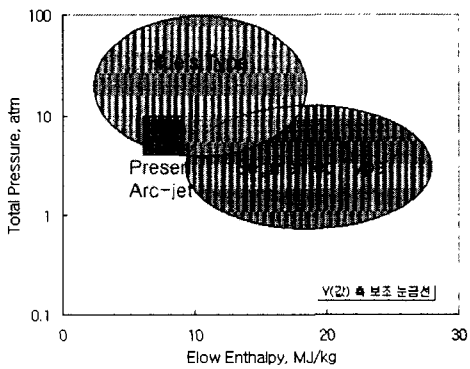

Fig. 5(d) Operating envelope of the present device

3. Calculation of flow characteristics

3.1 Nozzle flow

Even though the present device is seen to produce enthalpy and temperature of significant magnitude, one must additionally determine how high heat transfer rates it can produce to a body placed at the exit plane of the nozzle. The flight regime of a typical launch system produces a heating rate in excess of 100 W/cm^2. Also, when the device is used for material synthesis, there will be radiative cooling of the object material by near-black body radiation. The heating rate produced by the arc-jet must overcome the radiative cooling rate. That is, the temperature at which the convective heat transfer rate is balanced by the black body radiation of the blunt body, i.e., the equilibrium surface temperature, must be higher than the vaporization temperature of the material being processed.

The heat transfer rate of interest is that to the stagnation point of a blunt body. The stagnation region of a blunt body can always be represented by a spherical surface of a certain nose radius. In the present work, the effective nose radius is taken to be 3 mm which is the largest practical radius to be tested with the 9 mm-exit diameter nozzle.

In order to determine the heat transfer rate to the stagnation point of such a blunt body, one must first know the thermodynamic conditions of the flow produced by the device. For this reason, an approximate calculation was made of the flow processes in the nozzle assuming the flow to be inviscid and one-dimensional.

It is well known that a nozzle flow in an arc-jet facility is in thermochemical nonequilibrium[5]. Nonequilibrium occurs usually at a point slightly downstream of the throat. For this reason, the flow is assumed to be in equilibrium to a point of area ratio 1.02. The nonequilibrium region is calculated using the well-known two temperature model. An axisymmetric hyperbolic geometry is assumed for the nozzle, i.e.

$$\frac{A}{A^*} = 1 + (x\tan\Theta / r^*)^2 \qquad (4)$$

where the half-cone angle Θ is 12 degrees. A chemistry model involving 5 chemical species(O, N, O_2, N_2, and NO), vibrational relaxation[6], and 12 chemical reactions[7, 8] listed in Table 1 and Table 2 are used.

Table 1 Vibration relaxation data

Species	C_p/R	Vibration mode	g	ω_e
O	2.5	0	1	
N	2.5	0	1	
O_2	3.5	1	1	1580.19
N_2	3.5	1	1	2358.57
NO	3.5	1	1	1904.10

Table 2 Reaction formular and their reaction rates, $k_f = AT^n exp(-C/T)$

Reaction	M	A	B	C
Thermal dissociation by heavy particle				
$O_2+M \rightarrow O+O+M$	O	5.09E18	-1.10	59360
	N	5.09E18		
	O_2	5.09E18		
	N_2	5.09E18		
	NO	1.27E19		
$N_2+M \rightarrow N+N+M$	O	3.00E22	-1.6	113200
	N	3.00E22		
	O_2	7.00E21		
	N_2	7.00E21		
	NO	7.00E21		
Exchange reactions				
$N_2+O \rightarrow NO+N$		5.09E12	0.42	42938
$O+NO \rightarrow N+O_2$		2.36E09	1.0	19220

For the one dimensional calculation, a steady-state one dimensional conservation equations are written in the form

$$\rho u A = \dot{m} = constant \quad (5)$$

$$\rho u \frac{du}{dx} = -\frac{dp}{dx} \quad (6)$$

$$H = h_t + h_v + h_r + h_o + \frac{1}{2}u^2 = constant \quad (7)$$

The rate of change of species mass fraction is expressed as

$$\rho u \frac{d\chi_i}{dx} = \dot{w}_i \quad (8)$$

Landau-Teller type equation [[6] is used to calculate vibrational temperature.

Figure 6, and 7 show the calculated nozzle flow parameters and species concentrations for a typical operating condition of settling chamber pressure of 10 atm and mass averaged enthalpy of 7 MJ/kg.

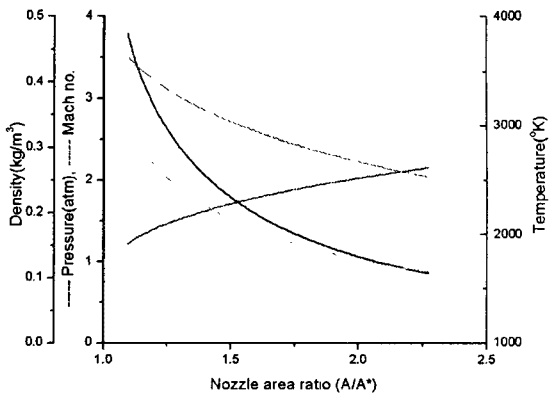

Fig. 6 Flow parameter distribution alon the nozzle axis

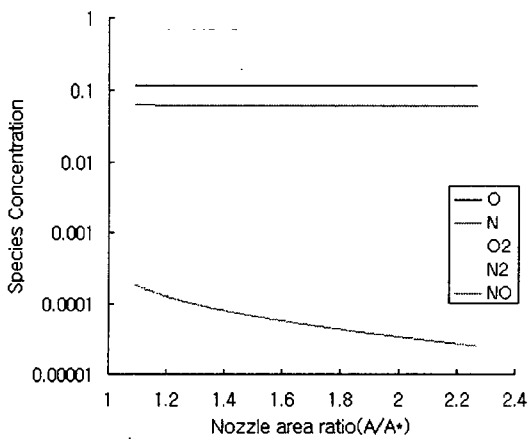

Fig. 7 Species concentration along the nozzle axis

As seen here, static pressure at nozzle exit is nearly atmospheric and there is significant dissociation of O_2: mol fraction of O is almost 15% for this case. Mach number is about 2.3 at the nozzle exit.

3.2 Post shock flow

In order to calculate the heat transfer rate to the stagnation region of a blunt body, one must know the flow conditions at the edge of stagnation boundary layer. It is well known that the flow reaches thermochemical equilibrium at the outer edge of a boundary layer in the stagnation region. But one must first determine this equilibrium condition at the edge of stagnation boundary layer.

In determine the equilibrium condition at the edge of stagnation boundary layer, one must account for the pressure rise from behind the shock wave to the edge of stagnation point boundary layer, where velocity is practically zero, because of the adiabatic compression process in the flow. This was accomplished by integrating the momentum equation

$$\frac{dp}{d(u^2/2)} = -\rho \qquad (9)$$

starting from the post-shock condition. The post shock condition is obtained in turn from the Rankine-Hugoniot relation for a frozen flow. The calculation results are given in Figs. 8, 9, and 10. The nozzle exit condition for the calculation is listed in Table 3.

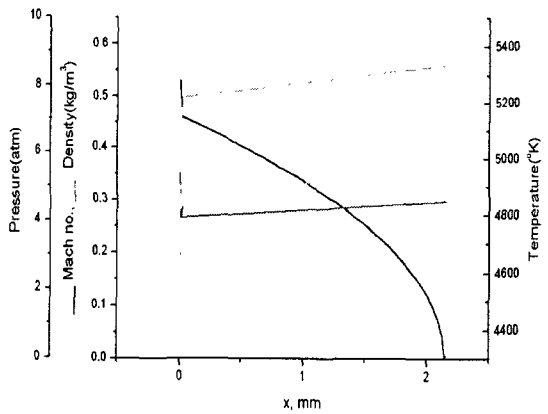

Fig. 8 Flow parameter distribution in the post shock flow region.

One sees here that the stagnation temperature reaches 6000 K and degree of dissociation of oxygen exceeds 30%. Stagnation pressure is approximately half of the settling chamber pressure. For the settling chamber pressure range of 4 to 10 atms, stagnation pressure (pitot total pressure) will be between 2 and 5 atms.

Table 3 Nozzle exit conditions for post shock flow calculation

u (m/s)	p (atm)	Mach	T (°K)	Density (kg/m^3)
2298.3	0.857	2.24	2577.5	0.108

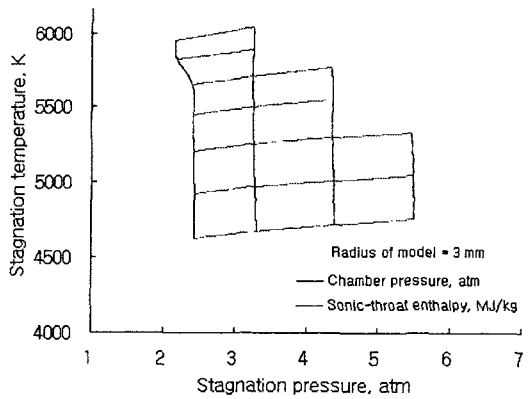

Fig. 10 Stagnation temperature distribution at the stagnation point

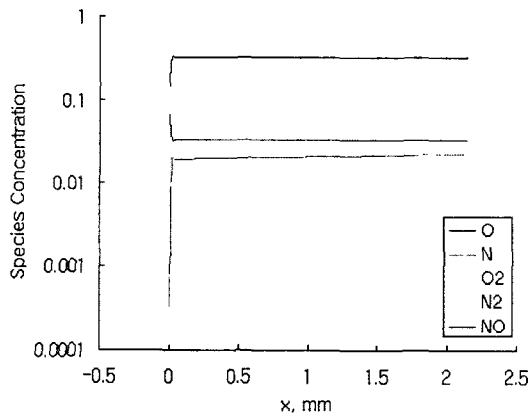

Fig. 9 Species concentration of atoms in the post shock flow region

3.3 Stagnation point heat transfer rate

The Fay-Riddell stagnation point heat flux equation[9] is used to estimate the desired heat flux at the specified stagnation point pressure, i.e.

$$\dot{q}_0 = 0.763\sigma^{-0.6}(H_e - h_w)\sqrt{\rho_e \mu_e \left(\frac{du_e}{dx}\right)} \qquad (10)$$

The stagnation point velocity gradient du_e/dx is determined from the Newtonian approximation

$$\frac{du_e}{dx} = \frac{1}{r_b}\sqrt{\frac{2p_e}{\rho_e}\left(1 - \frac{p_1}{p_e}\right)} \qquad (11)$$

The viscosity is taken to be

$$\mu_e = 1.819 \cdot 10^{-5}\left(\frac{T_e}{298}\right)^{0.8} \quad N \cdot s/m^2 \quad (12)$$

The cold-wall heat transfer rate, i.e. the condition where h_w=0, is shown in Fig. 11. As shown, the expected heat transfer rate reaches 300 W/cm^2, which should be adequate for most applications.

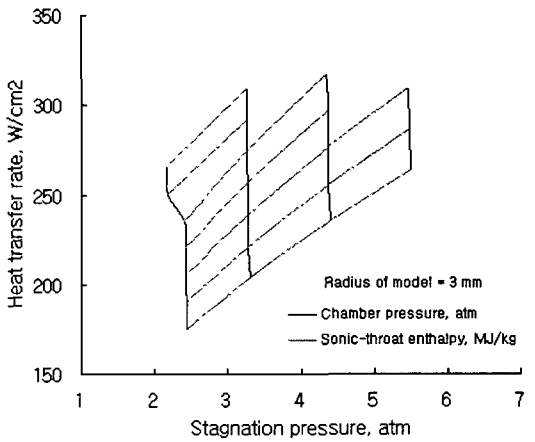

Fig. 11 Heat transfer rate at the stagnation point

As mentioned, radiation-equilibrium temperature at the stagnation point must be known. When the sample reaches a state of radiative equilibrium, the aerodynamic heat flux delivered to the sample is balanced by the black body radiation flux

$$\dot{q}_0 = 5.679 \cdot 10^{-12} T_w^4 \quad (13)$$

The heat transfer rate under this condition is known as hot-wall heat transfer rate. It is determined by the iteratively coupled calculation of Eq.(10) and Eq.(13). The calculated equilibrium temperature distribution is shown in Fig. 12. As seen the radiation equilibrium temperature reaches 2700 K. Thus, the present device should be capable of synthesizing material with vaporization temperature below 2700 K.

4. Discussion

As mentioned, the sonic-throat method of determining enthalpy is applicable strictly to an inviscid one-dimensional flow. As mentioned, the sonic-throat enthalpy is found to be nearly equal to the heat-balance enthalpy which is a mass-averaged enthalpy. Because of the boundary layer, the flow is never a one-dimensional flow: enthalpy is highest at the centerline and decreases toward the wall. All tests are conducted on a model placed at the centerline. At the centerline, flow enthalpy should be higher than the average enthalpy derived in the present work. That is, the ratio h_c/h_{av} varies from 1.4 to 4 [10, 11]. In this work, the mass averaged enthalpy at the stagnation point is calculated to be between 9 to 13.5 MJ/kg. The stagnation point enthalpy of the presnt 150 kW arc-jet at the centerline of flow is likely to be more than 15 MJ/kg. This device seems to be effective in testing

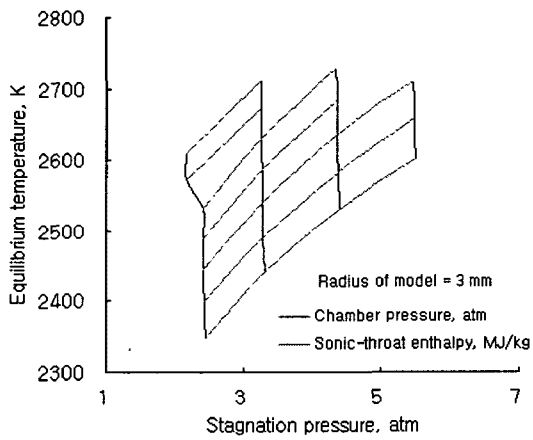

Fig. 12 Equilibrium temperature distribution at the stagnation point

heat-resistant materials for space launchers and in synthesis of high temperature materials such as diamond. Effort is being made presently to determine the centerline enthalpy using optical spectroscopy.

5. Conclusions

A newly designed and constructed 150 kW Huels type arc-jet produces an average enthalpy in the range from 9 to 13.5 MJ/kg at a settling chamber pressure in the range from 4 to 10 atm and stagnation pressure of 2 to 5 atm. Based on the average enthalpy, at the

stagnation point, the stagnation point heat transfer rate is predicted to be between 175 and 318 W/cm^2, and the gas temperature is predicted to be between 4630 to 6050 °K respectively' degree of dissociation exceeds 30%. If the centerline enthalpy, which should be higher than the average enthalpy but is presently unknown, is used, these values will be higher.

References

[1] R. K. Smith, D. A. Wanger, and J. Cummingham, "A survey of current Future Plasma Arc-Heated Test Facilities for Aerospace and Commercial Applications". AIAA Paper 1988-146-408, 1997.

[2] Rusian

[3] M. Hinada, Y. Inatani, T. Yamada, and K. Hiraki, "An Arc-Heated High Enthalpy Test Facility for Thermal Protection Studies", ISAS Report No. 664, 1996.

[4] W. Winovich, "On the Equilibrium Sonic-Flow Method for Evaluating Electric-Arc Air-Heater Performance", NASA TN D-2132, 1964.

[5] R. Matsuzaki, "Design of Contoured Nozzle for Arc-Heated Wind Tunnels", AIAA Paper 94-2593, 1994.

[6] Chul Park, "Nonequilibrium Hypersonic Aerothermodynamics", John Wiley & Son, New York, 1990.

[7] R. Oldenborg, et al., "Reaction Rates(Baulch) NASP", Status Report of the Rate Constant Committee, NASP High Speed Propulsion Technology Team, 1989.

[8] S. W. Baek and J. U. Kim, "Supersonic Flow of Hydrogen and Air in a Duct with Variable Area", KSME Journal, Vol. 6, No. 2, pp. 149~153, 1992.

[9] J. A. Fay, F. R. Riddell, and N. H. Kemp, "Stagnation Point Heat Transfer in Dissociated Air Flow", Journal of Aeronautical Sciences, Vol. 25, No. 2, 1958, pp. 73-97.

[10] A. F. Okuno and C. Park, "Stagnation-Point Heat-Transfer Rate in Nitrogen Plasma Flows: Theory and Experiment", ASME Journal of Heat Transfer. Vol. 92, Series C, No. 3, August 1970, pp. 372-384.

[11] Chul Park, "Comparison of the Enthalpy Determination Methods for an Arc-jet Facility", AIAA Paper 2004-487, 2004.